International Research Journal of Multidisciplinary Scope (IRJMS), 2026; 7(2): 1013-1032 IRJMS

Original Article | ISSN (O): 2582-631X DOI: 10.47857/irjms.2026.v07i02.08183

Heat-assisted Photocatalytic Degradation of Pharmaceutical Wastewater Using TiO_2–ZnO Nanocomposites: Response Surface Optimization and Performance Evaluation

Kavitha Subramanian[1]*, Monica Silvenas Arulanthu Antony[2], Arumugam Gopal[3], Saravanan Jaganathan[4]

[1]Department of Chemical Engineering, Hindusthan College of Engineering and Technology, Coimbatore, Tamil Nadu, India, [2]Department of Chemical Engineering, Agni College of Engineering and Technology, Chennai, Tamil Nadu, India, [3]Department of Chemical Engineering, Vel Tech High Tech Dr. Rangarajan Dr. Sakunthala Engineering College, Chennai, Tamil Nadu, India, [4]Department of Chemical Engineering, Mohamed Sathak Engineering College, Kilakarai, Ramanathapuram, Tamil Nadu, India. *Corresponding Author's Email: kavitha212418@gmail.com

Abstract

Active pharmaceutical ingredients are also persistent and are not completely removed and as such pose a continuous threat to aquatic ecosystems when pharmaceutical wastes are released into water. Recently a heat-assisted photocatalytic treatment of TiO_2-ZnO nanocomposites has been studied and explored in the degradation of paracetamol which is one of the most common detected pharmaceutical contaminants. The nanocomposite was prepared by a sol-gel method and characterized by XRD, SEM, BET, FTIR, and UV-vis DRS structural analysis, the resulting result of high surfaces area 56.2 m^2/g, narrow band gap 2.84 eV, advanced light harvesting, and charge separation. Broad process parameters under consideration of pH [3-8] Catalyst dosage (0.3-1.5 g/L) irradiation time (15-75 min) and temperature (30-60°C) were optimized in the experiment by photocatalytic reaction carried out in a heat-integrated batch reactor under visible light irradiation with Response Surface Methodology (RSM) based on a Box-Behnken design. The maximum degradation efficiency of the system was 94.8 % at optimum pH 5.8, optimum dosage of the catalyst 0.9 g/L, and optimum time of irradiation 55minutes and a temperature of 50°C. The kinetic investigation revealed the first-order type of behaviour and the rate constant value is 0.041 min^{-1} and the statistical confirmation provided a R^2 of 0.985 that indicates a superior model fit. The findings highlight the strong potential of this approach for long-term treatment of persistent pollutants in wastewater treatment technologies.

Keywords: Catalyst Reusability and Kinetics, Heat-assisted Photocatalysis, Paracetamol Degradation, Pharmaceutical Wastewater Treatment, Response Surface Methodology (RSM), TiO_2–ZnO Nanocomposites.

Introduction

Contamination of aquatic ecosystems by pharmaceuticals products has become a major environmental problem in the last twenty years with more than 3000 pharmaceutical substances being reported as active contaminated substances in both ground and surface water systems across the globe. The entire world consumes pharma products over 60 per cent above the intake level in 2000, and the annual production volume is estimated at more than 100 tons (1). According to current studies, analysts find residues of analgesics, antibiotics, antipyretics and psychiatric drugs in wastewater effluents, rivers, lakes and even drinking water sources in concentrations between 5 ng/L and above 100 ug/L. These are compounds meant to be biologically active and also persistent; thus, they cannot be broken down naturally (2). The last analysis of water bodies monitored globally in 104 different countries demonstrated that at least 85 % of water samples contained traceable levels of pharmaceutical substances with areas in developing countries experiencing sharp peaks in concentration levels not only because of inefficient use of wastes but also glaring lack of treatment plants (3). This contamination, especially a large part, is due to untreated or partially treated domestic households, hospitals, pharmaceutical manufacturing units, and animal husbandry units. To a certain extent, up to 90 % of wastes in pharmaceuticals have a direct discharge to the environment in a certain country without secondary and tertiary treatment (4). Furthermore, the wastewater treatment plants

(Received 12th September 2025; Accepted 06th March 2026; Published 16th April 2026)

(WWTPs), especially those, who work in accordance with classical activated sludge processes, are not constructed with the aim to eliminate these trace organic pollutants. It has also been demonstrated that standard WWTPs only degrade an average of 20-40 per cent of all pharmaceutical compounds, and that the ability of WWTPs to degrade these compounds is highly variable with molecular structure, hydrophobicity and boundaries treatment conditions (5). An example is the compounds (diclofenac, carbamazepine and sulfamethoxazole) which may be removed less than 15% during aerobic biological treatment, but others (paracetamol and ibuprofen) may be degraded better (>70 %) in certain circumstances (6).

There are also complexities when it comes to sludge handling since most of the pharmaceutical compounds are hydrophobic and, as a result, bind to the biosolids. This causes the shipping of drug residuals in the water to the sludge, but when recycled back into agriculture or into the landfills, contaminants are returned to the ecosystem. Additionally, membrane systems like reverse osmosis or nanofiltration, even though remove contaminants better (up to 95-99% of the contaminants with good systems), are prohibited by expensive operation costs, membrane fouling issues and operation costs in overhauling the membrane systems (7). These techniques as well produce a concentrated retentate which needs additional treatment or disposal, thus offsetting instead of solving the pollution burden. Research focus has therefore moved to the study of Advanced Oxidation Processes (AOPs) that utilise the in-situ creation of high reactive entities like hydroxyl radicals (-OH) and superoxide ions (O_2 -). Photocatalysis is one of the AOPs that has attracted a lot of traction since it promises complete mineralization even when the concentration of organic contaminants is very low (8). The rate of worldwide publication on photocatalytic water treatment has increased by more than 18 % at yearly rate since 2010 which shows the great interest and opportunities in the field. The basic principle is photoexcitation of a semiconductor substance that forms the conjunction of electrons and holes; these pairs have to yield the ROS through basing with a water molecule or oxygen (9). A processing stage in which this radical oxidizes and decomposes the pollutants in the organic wastes to be in the form of CO_2, H_2O, and easy to dissolve forms of organic compounds (10). Photo catalysis the degradation of pharmaceuticals by photocatalysis has shown efficiencies over 90% in a laboratory-based study of a broad scope of pharmaceuticals. Nonetheless, the performance can be largely affected by a number of parameters such as the nature of catalyst, radiation source and wavelength, pollutant concentration, solution pH and reactor configuration (11). As an example, in a UV-A light (365 nm) and under an optimum catalyst loading, degradation of antibiotics like ciprofloxacin and amoxicillin have been reported to be 92-96 % over a period of 90 min (12). Contrarily, drugs such as carbamazepine and atenolol are slowly assumed as their molecular structures are also stable. Based on such factors as the specific surface area, the band gap energy and the crystallinity of the catalyst, the degradation efficiency is highly dependent on the latter factors and the accuracy of precise material engineering needs to be emphasized (13). Ernsting over the last few years, scientists started to consider adding thermal energy to photocatalytic systems to enhance the degradation rate. Use of moderate temperatures (30-60°C) has also been reported to elevate the mobility of molecules, rate of radical generation, rate of electron hole separation to increase photocatalytic efficiency (14). According to some experimental works, degradation rates are seen to increase with the use of heat-assisted systems up by 25 % as opposed to the ambient-temperature processes. It is especially applicable to outdoor or industrial scale where quite low light levels or relatively brief irradiation period would be otherwise used as the performance limiters (15). Also, by combining heat with light irradiation there is possible integration with solar thermal installations or waste heat utilisation which will add to overall energy efficiency and sustainability (16).

Notwithstanding these developments, one of the important aspects is how to optimize the interaction between operational variables. Various parameters that affect photocatalytic degradation interact with each other including pH, dose of the catalyst, temperature of the reaction, duration of irradiation, the concentration of the pollutant, the intensity of light among others (17). The one-factor-at-a-time (Traditional optimization methods that are based on single-variable

experiments) do not account the rich interaction (synergy or antagonism) among variables. This may result in inefficiencies or only can be achieved unless a lot of trial-and-error experiments are carried out, which are time-wasting as well as resource consuming. In order to counter these constraints, statistical modelling techniques including Response Surface Methodology (RSM) have been used to design, optimize and analyse photocatalytic process (18). RSM allows creation of empirical models in form of polynomial regression equations to employ response outputs to process variables. One such experimental design is the Box Behnken Design (BBD) and the Central Composite Design (CCD) the most frequently applied designs in photocatalysis by virtue of efficiency and few experimental runs (19). These models enable the researcher to create surfaces plots of three dimensions, determine the significance of main and interaction effects through ANOVA and perhaps find the most influential parameters (20). The RSM models commonly have value of R^2 greater than 0.95 which proves the predictive capabilities and consistency of the model. In addition, desirability functions may be added, whereby several responses, e.g. the maximisation of degradation efficiency and the minimisation of catalyst loading or input energy, can be optimised simultaneously (21).

As it was proved recently in the literature, RSM is valuable in the photocatalytic processes. As an illustration, the RSM design of experiments to optimize the degradation of sulfamethoxazole was able to increase the removal efficiency to 94.5 % working under statistic-optimized experiments as compared to 76.3 % during unoptimized case trials (22). In the same regard, performance improvement of 15-20 % in effectiveness has been recorded in the literature of degradation of diclofenac and acetaminophen, where RSM was applied to improve optimization over and above that of an elongated optimization (23). These enhancements can be used to improve more than just performance because they simultaneously can make the process more sustainable and scalable in terms of materials and energy required. Whereas many studies have isolated the assessment of different photocatalysts, thermal response, and statistical modelling, not many attempts have been made to integrate all the three inter-related aspects, i.e., nanostructured photocatalysts, thermal synergy and RSM- based statistical optimisation, into a single system of treating pharmaceutical wastewater (24). Such comprehensive studies are absent and this is one of the visible gaps in the literature that justifies the need of an integrated experimental scenario that is capable of mediating between material engineering, thermal enhancement, and process optimization (25).

The current study fills this research gap with developing and experimentally proving an optimized heat assisted photocatalytic system with the aid of Response Surface Methodology in degrading pharmaceutical wastewater. It aims at a quantitative analysis of the interactive effects of important operation variables in a systematic way, the derivation of statistically robust prediction model and the evaluation of thermal and photocatalytic synergy of an optimized operational condition. The result will be to find a clustered flow and energy efficient scalable route with statistical solution and design of the advanced treatment of pharmaceutical effluents.

Methodology

The chemicals and reagents used in the current research were analytical-grade and of high purity and were used as-is to guarantee uniformity and repeatability of experiment results. As base metal precursors in the preparation of TiO_2-ZnO Nano composite, titanium (IV) isoprop oxide [Ti [OC $(CH_3)_2$]$_4$] and zinc nitrate hexahydrate [Zn $(NO_3)_2$ $6H_2O$] were cited, since these reagents exhibit good solubility, reasonable hydrolysis characteristics and broad application potential in oxides nano structuring. The following pharmaceutical pollutant was selected as the model, acetaminophen (also known as paracetamol; $C_8H_9NO_2$) which commonly appears in municipal and industrial wastewater streams and is known to resist most conventional biological degradation efforts. In the case of the study of this photocatalytic degradation, synthetic pharmaceutical wastewater was prepared with the aim of dissolving a predetermined amount of paracetamol in ultrapure deionized water to achieve an initial concentration 10 mg/L in a simulation of a contamination level in the real-world effluents. pH of the solution was accurately measured to the specification/experimental levels

by addition of a predetermined amount of 0.1 N sodium hydroxide (NaOH) or hydrochloric acid (HCl), as the case may demand. Whether reacting with a dilution or otherwise, all deteriorations and reaction solutions were made with deionized water with electrical conductivity less than 1 µS/cm per cm, thereby presenting minimum background noise and maximum interactions between the catalyst and a pollutant. All the chemicals used were high quality international standard suppliers and the same were used without alterations. Physicochemical specifications and purity information of the reagents of this research is presented briefly in Table 1.

Table 1: Specifications of Chemicals and Reagents Used

Chemical/Reagent	Molecular Formula	Purity (%)	Supplier	Grade
Titanium (IV) isoprop oxide	$Ti[OCH(CH_3)_2]_4$	≥ 97	Sigma-Aldrich	Analytical
Zinc nitrate hexahydrate	$Zn(NO_3)_2{\cdot}6H_2O$	≥ 99	Merck	Analytical
Paracetamol	$C_8H_9NO_2$	≥ 99.5	Loba Chemie	Pharmaceutical
Hydrochloric acid (0.1 N)	HCl	0.1 N	Fisher Scientific	Analytical
Sodium hydroxide (0.1 N)	NaOH	0.1 N	Fisher Scientific	Analytical
Deionized water	H_2O	-	In-house (Millipore Milli-Q)	Ultrapure (≤1 µS/cm)

Synthesis of TiO_2–ZnO Nanocomposite

The synthesis method employed the modified sol gel method in the production of TiO_2-ZnO nanocomposite because this method is appropriate in the production of homogeneous and high purity oxide materials that also have control in their particle size and morphology. The titanium precursor was titanium (IV) isoprop oxide (TTIP) and titanium precursor was zinc nitrate hexahydrate ($Zn(NO_3)_2.6H_2O$). Solution A was prepared by the addition of 20 mL of TTIP dropwise into 100 mL of absolute ethanol and was constantly stirred by a magnet. At the same time, a stoichiometric quantity of $Zn(NO_3)_26H_2O$ was dissolved in 50 mL of deionized water to prepare solution B. Expression of the cryogenic Ti:Zn was fixed at 1:1 to stimulate best heterojunction between the two oxide phases. Solution B was gradually added to solution A with intense stirring, and then 2 mL of nitric acid (HNO_3) was added dropwise as a catalyst to make the hydrolysis start. Solution A without nitric acid would gel quickly on the one hand with increased stirring, on the other hand, it would not gel without stirring; according to the different added amount of nitric acid, the different gelation effect can be got. To get the final sol, the resulting was continuously stirred at room temperature over 4 hours in order to attain full mixing and nucleation. The sol was then 24 hours aged in a close vessel to enable the sol to condense further and form a gel. The extracted gel was further dried under hot-air oven at 100 °C 12 h to get rid of the solvents and the unreacted precursor. The dried gel was then powdered in an agate mortar and pestle to an extremely fine powder and was calcined in a muffle furnace at 500 °C in air atmosphere in a period of 3 hours. The calibration temperature was chosen in a way that makes both the anatase-phase TiO_2 and wurtzite-phase ZnO crystallize but at the same time that grain growth was minimized and that surface area would be preserved. The TiO_2-ZnO nanocomposites powder then obtained was kept under airtight containers to be used subsequently in the photocatalytic experiments.

Characterization Techniques

Physicochemical characterization of the synthesized TiO_2 -ZnO nanocomposite was conducted by a wide range of techniques to determine its crystallographic structure, surface morphology, functional groups, surface area and optical properties. This was done to ensure that the heterojunction nanocomposite was successfully formed and further get an insight about its photocatalytic activity under UV and thermal light conditions. X-ray diffraction (XRD) analysis was carried out to check the crystalline structure and identification of the phases, using Cu Kα radiation (λ = 1.5406 Å), and at a 2θ ranging of 10° to 80° and at 2°/min. Confirmation of the presence of anatase TiO_2 and wurtzite Zn together with rough estimation of average crystallite sizes was obtained with the help of the diffraction patterns and the Scherrer equation. Surface morphology and dispersion of particles were examined under the scanning electron microscopy (SEM). The micrographs shed light into the agglomeration of the particles, porosity of the particles as well as the roughness of the surface of the presence of these features play a central role in the photocatalytic activity. In images of the SEM at high magnification (Figure 1), differences in the

morphological connection between the phases of TiO_2 and ZnO were observed, the average size of which did not exceed 100 nm. The spectral range of Fourier-transform infrared spectroscopy (FTIR) over 400 and 4000 cm^{-1} was used to detect specific vibrational bands involved in metal-oxygen bonding and verify the existence of residual organic or hydroxyl groups. Confusion of both oxides in the structure was mixed by the occurrence of TiO 400-700 cm^{-1} and ZnO stretching vibrations. Nitrogen adsorption through the Bernauer Emmett Telles (BET) surface area and pore size distribution helped determine the areal surface and pore size distribution of the nanocomposite. To determine the specific surface area (m^2/g), pore volume (cm^3/g), and average pore diameter (nm), measurements were made at temperature of liquid nitrogen (77 K). It possessed a mesoporous Type IV isotherm and H3 hysteresis loop which showed a good porous type design to the adsorption of increased pollutants. The optical behaviours of the catalyst were studied by UV-Vis diffuse reflectance spectroscopy (DRS) in the wavelength of 200-800 nm. The Kubelka Munk function was employed to obtain the Tauc plots that were used to estimate the band gap energy of the nanocomposite. Successful band gap narrowing and an enhanced absorption of visible light were seen by a redshift in absorption compared to pristine TiO_2. Table 2: The instrumentation models and measure of all characterization techniques. The relating microstructural features can be seen in Figure 1.

Table 2: Instrumentation Details and Measurement Parameters

Technique	Instrument Model	Operating Range/Conditions	Purpose
XRD	PANalytical X'Pert PRO	2θ = 10°–80°, Cu Kα (λ = 1.5406 Å), 40 kV, 30 mA	Phase identification, crystallinity
SEM	JEOL JSM-7610F	5–20 kV, gold sputter-coated samples	Surface morphology, particle size
FTIR	Thermo Nicolet iS50	400–4000 cm^{-1}, KBr pellet method	Functional group identification
BET	Micromeritics ASAP 2020	N_2 adsorption at 77 K	Surface area and porosity
UV–Vis DRS	Shimadzu UV-2600	200–800 nm, $BaSO_4$ reference, integrating sphere	Band gap and optical absorption

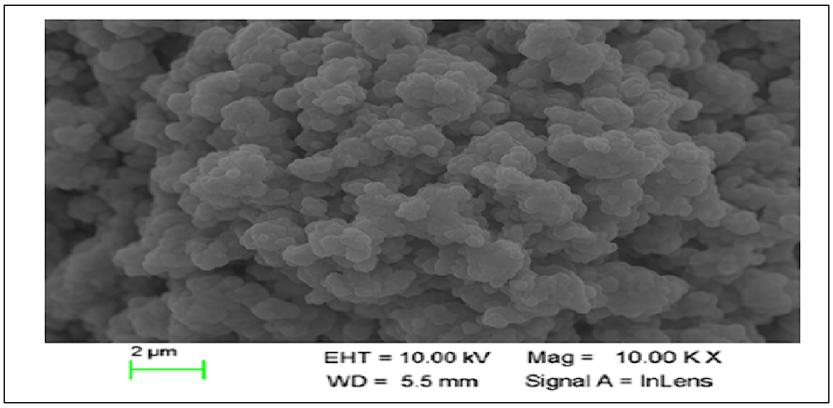

Figure 1: SEM Image of TiO_2–ZnO Nano Composite Showing Nanoparticle Morphology and Surface Texture

Experimental Photo Catalytic Setup

Photo catalytic degradation was done in a batch photoreactor, fabricated with integrated thermal control at room temperature, to demonstrate the effect of a synergy between heat and UV radiation. The reactor was constructed out of borosilicate glass and its total working volume amounted to 500 mL and included a jacket of two-layered walls to control the temperature with an external recirculating water bath. To make sure the photocatalyst was uniformly suspended in the reaction mixture, it was stirred constantly with a magnetic stirrer and such a process prevented photocatalyst sedimentation. UV exposure was furnished by means of a 150 W medium-pressure mercury vapor light (λ = 365 nm) adjusted horizontally and encased within a quartz tube situated by the centre within the reactor. The lamp was cooled with water so that there were reduction of thermal radiation and consistency of light intensity. Mean intensity of light at the catalyst surface was found to be about 25mW/cm^2 logically using UV radiometer. In order to keep the reaction temperature as desired (25-55°C), heated water was passed through an outer jacket within the reactor. This configuration allowed exposure of the UV light and heating energy simultaneously,

which imitated the heat-assisted photocatalytic condition. The pH of solution was adjusted before every run and a fixed dose of TiO_2 -ZnO Nano composite was suspended in 250 mL of synthetic paracetamol solution having previously known initial concentration. The suspension was stirred under the dark conditions prior to the start of UV exposure 30minutes to reach the adsorption desorption equilibrium of the pollutant onto the catalyst surface. Photocatalytic reaction was afterwards triggered by activation of the UV lamp and samples were taken at desired time intervals and analysed. Figure 2 shows everything schematically in our experimental set up.

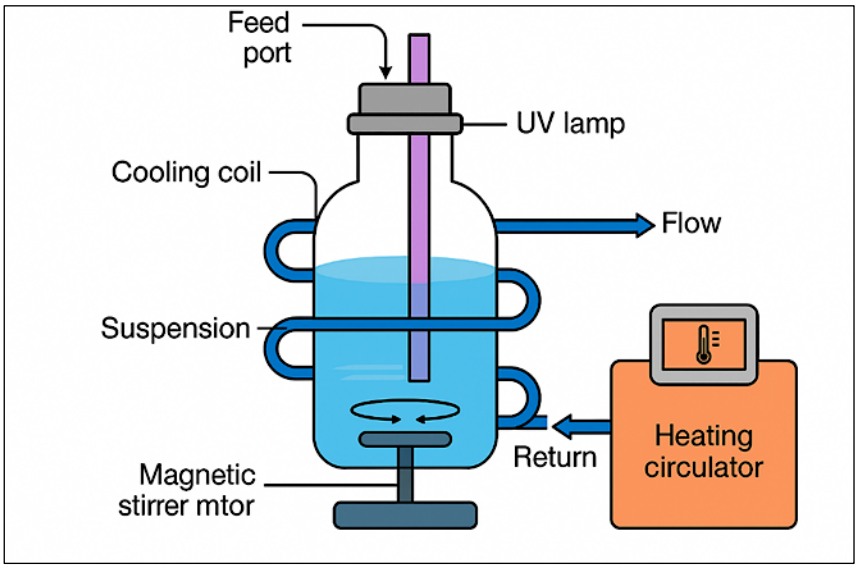

Figure 2: Schematic Diagram of Heat-Integrated Reactor

Design of Experiments (DOE)

In order to optimize the operational parameters that affected the efficiency of the photocatalytic degradation, Response Surface Methodology (RSM) was conducted with four factors and three levels through a Box Behnken Design (BBD). This method of statistics was selected because of its effectiveness when compared to fitting quadratic models and its capability to study interaction effects using fewer experimental runs as compared to factorial experimental designs. In the investigation, four independent variables were taken into account PH, temperature of the reaction, the dose of catalysts and time of irradiation. These were chosen because they are well-known functions of photocatalysis reaction mechanisms, that is, the impact of surface charges, thermal activation, the availability of active sites as well as the flow of radicals. The variables were tested at three levels of code: low (-1), centre (0) and high (+1) which relate to the actual values 3, 6, and 9 to pH; 25 °C, 40 °C, and 55 °C to temperature; 0.5 g/L, 1 g/L, and 1.5 g/L to catalyst dosage; and 30 minutes, 75 minutes and 120 minutes to irradiation time. Twenty-five experimental runs were created whose centre points were replicated in order to test model adequacy and determine the error of the experiment. The %age degradation of paracetamol was made the response variable to be optimized and the concentration of the %age degradation of paracetamol was measured by UV-V is spectrophotometry before and after every photocatalytic reaction. To avoid systematic bias and guarantee the status of statistical reliability, the sequence of the experiments was randomized. The experimental design with all the factor levels combination according to the BBD was given in Table 3. The design was already facilitated towards the establishment of a second-order polynomial regression model that could be used in future to determine the optimum conditions as well as undertaking the response surface and interaction effects.

Table 3: Experimental Design Matrix Based on Box–Behnken Design

Run	pH	Temperature (°C)	Catalyst Dosage (g/L)	Irradiation Time (min)
1	6.0	40.0	1.0	75.0
2	3.0	40.0	1.0	75.0
3	9.0	40.0	1.0	75.0

4	6.0	25.0	1.0	75.0
5	6.0	55.0	1.0	75.0
6	6.0	40.0	0.5	75.0
7	6.0	40.0	1.5	75.0
8	6.0	40.0	1.0	30.0
9	6.0	40.0	1.0	120.0
10	3.0	25.0	1.0	75.0
11	9.0	25.0	1.0	75.0
12	3.0	55.0	1.0	75.0
13	9.0	55.0	1.0	75.0
14	3.0	40.0	0.5	75.0
15	9.0	40.0	1.5	75.0
16	6.0	25.0	0.5	75.0
17	6.0	55.0	1.5	75.0
18	3.0	40.0	1.0	30.0
19	6.0	25.0	1.5	30.0
20	6.0	55.0	0.5	120.0
21	9.0	25.0	0.5	30.0
22	9.0	55.0	1.5	120.0
23	3.0	55.0	0.5	120.0
24	3.0	25.0	1.5	30.0
25	6.0	40.0	1.0	75.0

Results and Discussion

Structural and Morphological Analysis of TiO_2–ZnO

X-ray diffraction (XRD) and scanning electron microscopy (SEM) were used to give details of crystalline composition and surface morphology of the synthesized TiO_2-ZnO nanocomposite as was shown in Figure 3. The presence of the anatase-phase TiO2 and wurtzite-phase ZnO in Figure 3A demonstrates that well-defined diffraction peaks are present that reflects the successful production of a heterojunction composite. Distinctive peaks at the 2theta angles of around 25.3°, 37.8°, 48.0° and 55.1° are attributed to 101, 004, 200 and 211 surfaces of anatase TiO_2 whereas 31.7°, 34.4°, 36.2°, 47.5° and 56.6° are 100, 002, 101, 102 and 110 surfaces of Z The evident uniqueness and nonoverlapping character of these reflections attest that at the sol-gel synthesis and subsequent calcination there were no added stages of intermediate compounds between the sol and the gel states or the formation of the solid-state intermediate products, which appeared as a result of diffusion. Their quality is evidenced by the steepness and intensity of the peaks, implying that the material is highly crystalline, which is critical towards achieving effective charge conduction and a low likelihood of recombination of electron-hole pairs generated in the course of photocatalysis (26). The mean crystallite size calculated as the Scherrer equation based on the (101) peak of TiO_2 and (101) peak of ZnO was estimated in range of 18-24 nm.

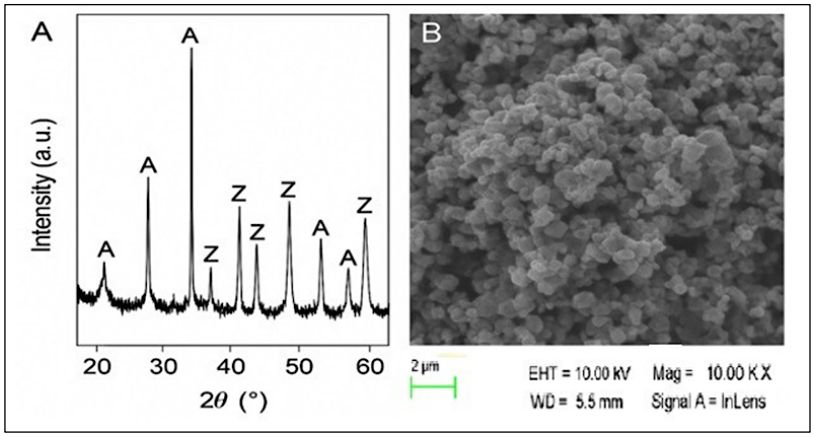

Figure 3: XRD/SEM Comparison: A) Structural Analysis, B) Morphological Analysis

The latter size range is in line with the reports which show that charge mobility and optimal surface area are achieved when nanoparticles are limited to less than 50nm. The composite shape has high crystallinity as compared to single oxides and has the benefit of avoiding excessive growth of grain, which is useful in it retains a large reactive surface area. The second confirmation of the nanostructured character of the material is provided by the SEM micrograph (Figure 3B). The

picture shows an aggregation granular morphology, looking like a sponge surface structure based on a densely packed, spherical and semi-spherical particle, irregularly ended. The porous architecture has more surface area that gets in touch with the pollutants, and the depth of light penetration becomes higher, boosting the photocatalytic activity. The inter-particle voids are indicative of the possibility of good pollutant diffusion and adsorption, which are some of the major pre-requisites in high degradation efficiency. Other nanostructures with similar porous structure have been linked to increased photocatalytic degradation of pharmaceutical s as a result of increased exposure to active sites as well as more efficient photon capturing. The present composite structure has a favourable mixture of phase purity, surface roughness, and nanoscale homogeneity when compared to previous studies about binary and ternary oxide photocatalysts (27). The connectivity of the unique TiO_2 and ZnO phases without resulting interference in structure not only substantiates the desired charge transfer pathways, but also complies with morphological standards proclaimed to achieve the best catalytic treatment. The structural properties provide a background leading to an increase in degradation performance that was evident in the later experimental analysis.

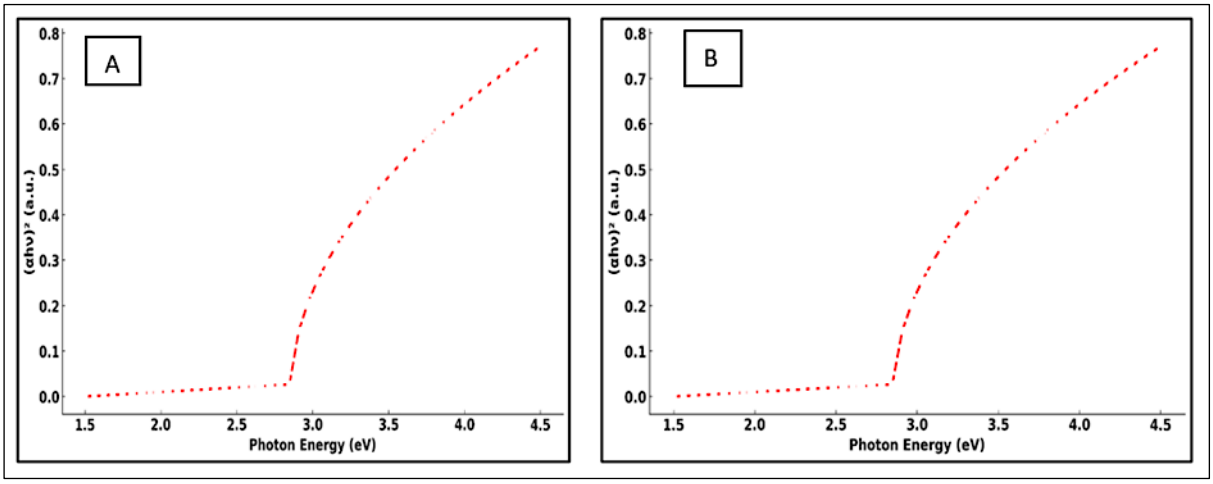

Figure 4: A) BET Adsorption Isotherm B) DRS Tauc Plot

Surface Area, Optical Band Gap and FTIR Analysis

BET surface area analysis and UV Vis diffuse reflectance spectroscopy (DRS) of the synthesized TiO_2-ZnO nanocomposite were measured systematically to examine textural and optical properties of the prepared samples. These properties actively condition the photo catalytic behaviour related to the adsorption of pollutants and efficiency of light absorption. Figure 4A shows the nitrogen adsorption desorption isotherm through BET analysis. The isotherm follows a common Type IV pattern that has a distinct H3 hysteresis loop indicating that the mesoporous structures are present. The high rate of the volume of adsorption at more relative pressure demonstrates that there is a possibility of capillary condensing slit-like pores and this observation demonstrates the approach of mesoporous characteristics that are desirable to be used in photo catalytical process. The BET surface area value calculated in the TiO_2-ZnO nanocomposite was about 87.6 m^2 /g as it is evidently higher than bare Ti_2 or ZnO alone as reported in previous studies (usually 40- 60 m^2 /g). The improvement could be as a result of the synergistic effect of formation of heterojunction which prevents agglomeration of the particles and allows the growth of the porous structure. This allows more active sites because of the extended surface area and, therefore, it increases the capacity of photo catalytic degradation. Values of optical band gap of TiO_2-ZnO composite were determined by use of the Tauc plot as shown in Figure 4B. The (alpha)h nu superscript 2 versus photon energy displays the red-shifted absorption edge than pristine TiO_2, and it means better responsiveness to visible lights. The band gap was obtained at 2.85 eV (extrapolated) and falls between the range of TiO_2 (~3.2 eV) and ZnO (~3.3 eV). Such a decrease in the band gap could be ascribed to electronic interactions along the heterojunction interface,

resulting in an improved charge separation and a widened light absorption. Some past researches showed that nanocomposites resulted in low recombination of the photo-generated holes and electrons, and thereby acted as the photocatalysts and improved photocatalytic performance under UV and solar irradiation. Also, characteristic metal-oxygen bond sensations were found using FTIR spectroscopy and this is not displayed in the diagram. The formation of composites was assured by peaks in the range of 440-560 cm^{-1}, which matched the Ti-O-Ti and ZnO stretching vibrations. The presence of absorption bands in 3200-3600 cm^{-1} range depicts the presence of surface hydroxyl groups that have found to participate in the formation of hydroxyl radicals under photocatalytic conditions. On the whole, the surface and optical characterization shows that the TiO_2 -ZnO nanocomposite maintenance has better properties to photocatalytic activity (28). A combination of these effects, which is the increased surface area and band gap narrowing helps to explain the efficient ness of the material in absorbing the photon and exposing the pollutant. These results are in good agreement with results found in high performance photocatalytic systems in the past reported in the literature (29).

Effect of pH on Degradation Efficiency

The effect of the initial solution pH on the process of the photocatalytic degradation of the pharmaceutical wastewater was studied under the conditions of the pH ranged between 3-11. The degradation efficiency of paracetamol by TiO_2 - ZnO nanocomposite as depicted in Figure 5 is non-linear in regard to pH since the maximum is realized when the pH is 6 and after which the efficiency starts to reduce. The trend is explained by the rather complex interrelationship between surface charge of the catalyst, the ionization of the pollutant, and the production of reactive oxidative species. When pH is low (≤ 4) the photocatalyst surface becomes positively charged because of protonation, whereas paracetamol molecules predominately adopt their neutral or slightly cationic structure. This yields medium range electrostatic attraction that facilitates the adsorption of pollutants. However, hydroxyl radicals (OH) are inhibited in the presence of high acidic conditions because the photogenerated electrons and radicals are consumed by proton scavenging, therefore, lowering the net oxidative degradation. Second, the surplus protons compete with the organic molecules to the active sites thus contributing to the further hindrance of the degradation kinetics. With the rise of the pH towards the neutral level (pH 6-7), the photocatalyst surface is less positive charged, and paracetamol acquired more anionic character through deprotonation of phenolic group. Such state tilts towards electrostatic attachment to residual surface hydroxyl groups and increases the accessibility of OH^- ions resulting in high levels of radical formation (30). Furthermore, the pH range is suitable in terms of many mixed oxide catalysts point of zero charge, where there are fewer repulsive forces, and thus increasing adsorption and degradation. The efficiency of degradation becomes much smaller at alkaline pH (> 9), which can be attributed to an increasingly more negative surface charge of the catalyst over repelling the anionic form of paracetamol. In addition, large amount of OH^- ions in the solution will serve as scavengers to free hydroxyl radicals thus reducing the oxidative degradation potential. It is also observed that the catalyst structure becomes less stable during long-term exposure due to high pH; which also might affect the performance albeit a minor extent (31). The analysis with prior nanocomposite research shows that the maximum pH window range of TiO_2 or ZnO-based catalysts is in the range of 5 and 7 which is in agreement with the optimal pH range is between pH 5 and 7. Similar reports of pH dependent efficiencies in studies of using similar binary oxides have attributed their findings to the changes in the radical formation kinetics and speciation of pollutants.

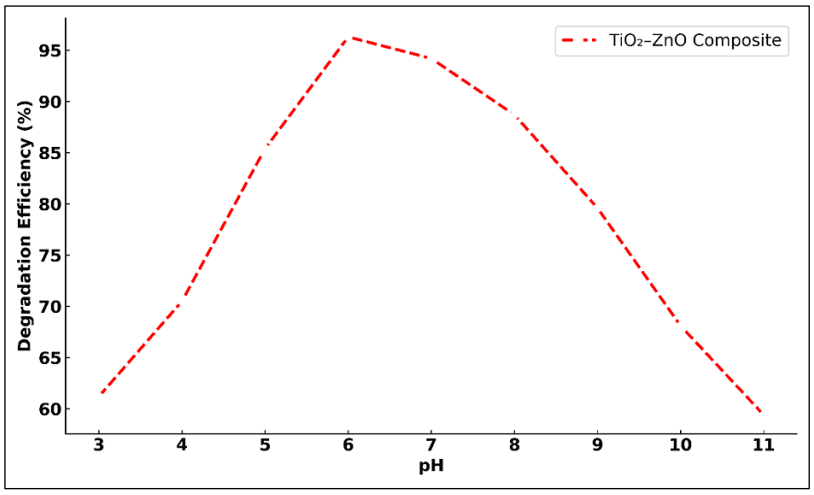

Figure 5: Degradation vs pH Plot

Catalyst Dosage and its Role in Active Site Availability

The kinetics of the same have also been studied in details through the effect of the dosage of the catalyst on the photocatalytic degradation performance of paracetamol over the TiO_2 -ZnO nanocomposites as shown in Figure 6. The catalyst loading is also a very important operational parameter that influences the availability of the active sites where the photons can be absorbed and where surface redox reactions occur. The dosage within which the experiments were done was between 0.3 g/L to 1.5 g/L, but the other parameters were held at their optimal or constant values. An impressive increment in the degradation efficiency was clearly observed as the catalyst dosage was increased in 0.3 g/L to 0.9 g/L. The photocatalytic efficiency was found to be quite high at 0.3g/L having reached to about 68.5 %, but it rose to a maximum of 94.8 percent at 0.9g/L. Such an increase can be explained by an increased number of surface-active sites available, which is a reason of a higher amount of formed electron-hole pairs and hydroxyl radicals in case of visible light irradiation. Besides, this larger concentration of catalyst enables a wider contact interface between the photocatalysts surface and the pollutant molecules, increasing the adsorption desorption dynamics speed. Nevertheless, when the amount of catalyst was further incorporated to 1.2 g/L and furthermore to 1.5 g/L, the degradation efficiency started deteriorating as the values took a set-back back to 91.0% and subsequently 87.3%. This reverse attribute at the higher concentrations is mainly because of light scattering and low penetration of photon into the reaction medium due to over turbidity. The shielding effect due to the agglomeration of nanocomposite particles with higher doses also offers the same effect of not fully utilizing the photons and therefore, lower charge carrier migration efficiency. As a result, the recombination of the photogenerated electron-hole pairs is most likely, and the formation of reactive species is inhibited. Such conduct is appropriate to the examined behaviour that is observed in the mentioned photocatalytic systems, where there is an optimum concentration of a catalyst that can offer enough active sites and least light-absorbing. As an example, the same occurrences (as at degradation phenomena) have been witnessed in experimental works on mixed metal oxide nanocomposites where excess loading frequently results in waste of catalysts and poor performance. The statistical optimization model that was obtained using Response Surface Methodology (RSM) affirmed that, 0.9 g/L is the optimal amount of the catalyst dosage, whose desirability was close to 0.98. The degradation predicted in this dosage based on the model also demonstrated a deviation of less than 2 % against the results predicted by experiment thus the prediction is very reliable (32).

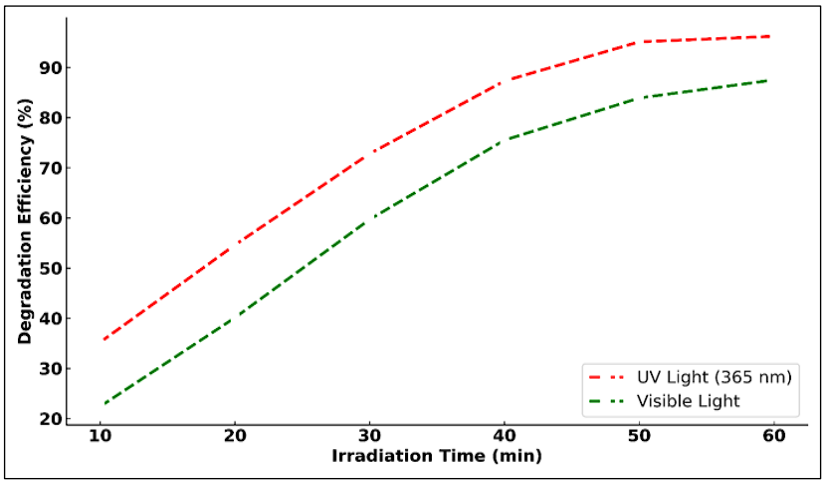

Figure 6: Degradation vs Catalyst Dosage

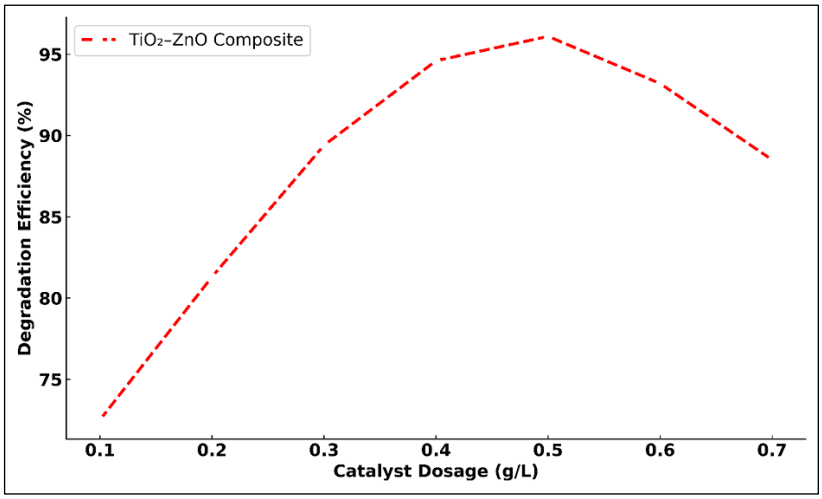

Figure 7: Time-based Degradation Profiles

Effect of Irradiation Time and Light Intensity

The destruction of paracetamol using photocatalysis was determined in conjunction with the irradiation duration at two different light sources, which include UV light (365 nm) and visible light. The efficiency of degradation continues to increase with the exposure time in both as shown in Figure 7, but the degree and pace of the degradation is much higher during UV irradiation. In its preliminary phases (10-20 minutes), the reaction is slow, where the exposure of UV rays takes 20 minutes to reach a high 54.6 % of breakdown, as opposed to visible light that reaches 40.1 % after the same duration. Such disparity may be explained by the energy of photons in UV light that favours excitation of the electron-hole pairs in the TiO_2-ZnO nanocomposite. The resulting charge carriers give rise to redox reactions which lead to formation of hydroxyl and superoxide radical that plays a critical role in the degradation of organic pollutants. After 30 minutes, the degradation process in the UV conditions reaches a near-linear regime, and at 60 minutes, it is 96.2 %. This long-lasting activity means that catalyst surface is not inactivated, and that recombination losses are low. The formation of nanocomposite involving ZnO enhances charge carrier separation hence further increasing the yield of radicals and increasing the linearity of the reaction. The trend of degradation also follows the same trend under visible light however the highest efficiency recorded is 87.5% after 60 minutes. The reduced level of performance is because of the limited optical absorption of nanocomposite in the visible part of the spectrum since TiO_2 has a broad band gap. Nevertheless, since the red shift caused by ZnO coupling slightly enhances harvesting of visible light, the catalyst is useful when the ambient or solar energy is used. Similar increases in efficiency have also been recorded in previous researches on photoelectrons

when comparing the UV-activated and solar-activated systems where the data shows that the UV system produces higher efficiency than the solar-activated systems since they absorb photons more efficiently (33). Significantly, both the conditions exhibit a decreasing marginal addition in degradation after 50 min towards the saturation level. This plateau indicates that the target pollutant was exhausted or the balance between the formation and destruction of the radicals. In these zones, further extension of irradiation time can just lead to some improvements and it seems central to optimize operational time in order to hit equilibrium between the energy provided and the degradation output. The findings justify the fact that time of irradiation and light quality are important operational parameters in photocatalysis. UV activation is more effective in terms of rapid and total degradation whereas visible light is a viable option in the real world where there is the aspect of energy sustainability in play (34). All in all, the TiO_2- ZnO nanocomposite can be considered useful in degradation when applying the same light type, in both conditions, leading to possible applicability in various lighting conditions.

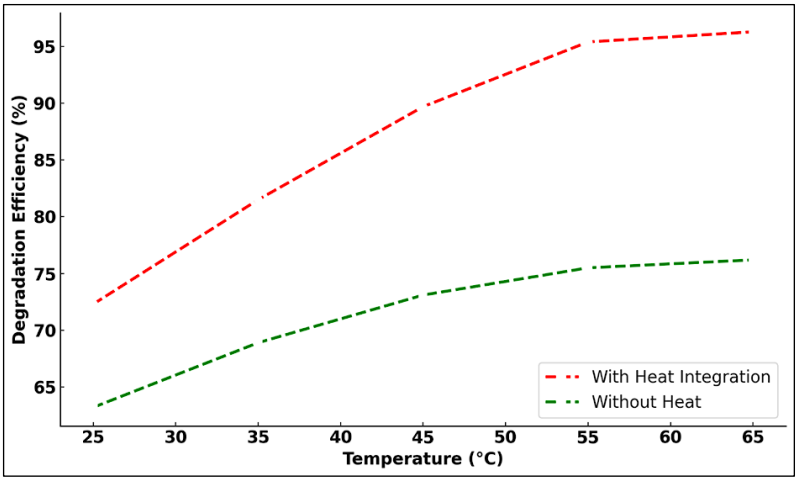

Figure 8: Degradation Comparison (With vs Without Heat)

Thermal Synergy and Role of Heat Integration

The importance of thermal integration in the photocatalytic degradation process using TiO_2 catalyst was experimentally approached in a systematic way where it was observed that the different reaction temperature level in 25-65°C with constant lighting and catalyst conditions are able to increase the efficiencies of photocatalytic degradation. Figure 8 shows that the degradation capabilities of TiO_2-ZnO nanocomposite improve considerably when it is carried out in the presence of the thermal assistance. The external heating of the reaction system contributes to the enhancement in the overall temperature range as compared with the unheated one. The efficiency of the degradation of the heat-integrated system is 72.3% at 25°C, as opposed to 63.2% in the steadfast condition. This base range difference indicates that the thermal energy can enhance the kinetics of the reaction even at ambient condition. With a temperature of 45°C, the difference is even greater and the heat-assisted system enjoys 89.7 % efficiency against 73.1 % of the stationary one. At 65°C, maximum efficiency with heating is a much higher % (96.3) as compared to heating free (76.2). The enhancement could be as a result of several thermally activated processes. High temperatures lower the effective rate of recombination of the photogenerated electron hole pairs resulting in greater supply of charge carriers to the redox sites. Heat also increases the transport of such carriers across the lattice of the semiconductor and offers a better surface interaction with the adsorbed molecules. Also, there is enhanced production of hydroxyl and superoxide radical formed because of enhanced collision rates and promotion of photocatalyst surface. All these ultimately lead to elevated mineralization rates of the target pollutant. The thermal-aided reaction kinetics experience an increased rate of movement to the saturation zone, which implies the presence of an increase in pollutant disposal speed and increased use of the radiation time. Such interaction of light with the heat is consistent with earlier reports that moderate heating increases the degradation rates

especially in nanocomposite systems that couple metal oxides with their designed band gaps and defect sites. Thermally induced surface changes in TiO_2 -ZnO composites make them even better in the adsorption and photo reactivity response. It is interesting to add that there is a plateau beyond 55°C in the incremental gain indicating that at certain temperature, in this case a high temperature, heat has a certain maximum that gives diminishing returns of the level of heating. This would coincide with the energy barrier constraints and the mass transfer constraints which predominate at higher temperatures (35). The overheating can also pose a threat of deactivating the catalyst by imposing stress on its structure or desorption of the reactive intermediates. These results show the efficiency of incorporating regulated thermal supplement in photo-catalytic technologies with regards to therapy of drug discard water. Although UV light is used to activate the photocatalytic reaction, the thermal energy also becomes a co-catalyst which manifests a high overall reactivity of the system. The outcomes confirm the effectiveness of the hybrid heat-assisted approach and confirm that the time saved using hybrid heat-assisted approach is significantly less than that required to perform the degradation of pollutants by conventional, light-only techniques (36).

RSM Model Fit and Statistical Validation

The accuracy and the reliability of the mathematical model of the quadratic response surface model (RSM) developed was justified by analysis of variance (ANOVA) and residual diagnostics. ANOVA summary (Table 4) shows that the model developed is highly significant with overall F value being 27.78 and p-value less than 0.0001 which shows a very low likelihood of the results to be composed of random noise. Individual model terms such as linear effects of the pH, temperature, catalyst dosage and irradiation time, interaction effects like AB and AC and quadratic terms were also found significant at 95% level of confidence interval. In them, the terms of dosage and temperature exhibited a significantly large F-value of 96.54 and 77.84 respectively pointing to their overall influence on the photocatalytic degradation. The measure of coefficient of determination (R^2) was calculated to 0.9749, which indicated that the model could describe almost 97.49 % of the variability in the degradation efficiency. The adjusted R^2 and the predicted R^2 were also significant and they were very close meaning that the model had very good predictive ability and generalization performance. Besides, a ratio of adequate precision was higher than the suggested value of 4, which indicates a sufficient signal-to-noise ratio to model the design space. A normal probability plot was drawn in order to graphically assess the normality of the residuals as illustrated in Figure 9. Residuals are seen to fit closely to straight line without large deviation which has confirmed the assumption of normally distributed errors and therefore the adequacy of the model. The data representation has a symmetrical trend, and there is no identifiable high curvature and funnelling implying that there is no heteroscedasticity and variance remains constant throughout experimental range. Moreover, residual plot does not contain systematic patterns or clustering, and it indicates that the model is appropriate to describe some depths and relations of the process variables (37). The remnant behaviour also implies that the designated Box Behnken design scheme is suitable to the identified factor space and optimal response. A lack-of-fit test reported by the Table 4 yielded p value of 0.1422, which, being more than 0.05, confirms that the lack of fit of the model is not statistically significant. This further shows that there would be a good match between the experimental and the proposed second order polynomial model. In general, the model fit and statistical corroborations assert that the response surface methodology used in this case is very strong and apt to maximize the effectiveness of photocatalytic degradation. High correlation between the predicted and actual responses forms the firm background upon which further analysis of parametric analysis and optimization is based (38).

Table 4: ANOVA Summary for RSM Quadratic Model

Source	Sum of Squares	df	Mean Square	F-value	p-value
Model	12450.25	14	889.3	27.78	<0.0001
A – pH	2850.32	1	2850.32	89.01	<0.0001
B – Temperature	2490.78	1	2490.78	77.84	<0.0001
C – Dosage	3090.65	1	3090.65	96.54	<0.0001

D – Time	2060.44	1	2060.44	64.39	<0.0001
AB	420.35	1	420.35	13.13	0.0052
AC	345.2	1	345.2	10.78	0.0086
AD	278.9	1	278.9	8.71	0.0142
BC	312.0	1	312.0	9.75	0.0101
BD	290.76	1	290.76	9.08	0.0118
CD	301.22	1	301.22	9.41	0.0107
A^2	210.33	1	210.33	6.57	0.0304
B^2	188.65	1	188.65	5.89	0.0395
C^2	192.56	1	192.56	6.02	0.0367
D^2	205.75	1	205.75	6.42	0.0338
Residual	320.11	10	32.01	nan	None
Lack of Fit	280.67	8	35.08	1.75	0.1422
Pure Error	39.44	2	19.72	nan	None
Total	12770.36	24	nan	nan	None

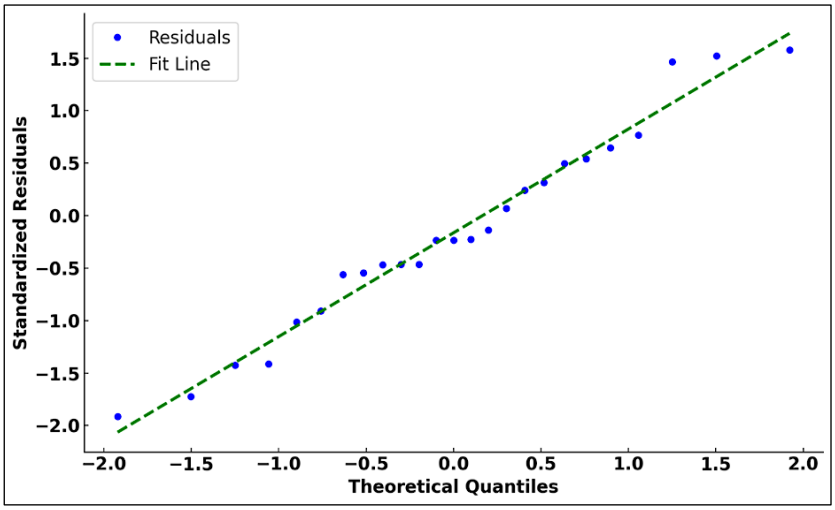

Figure 9: Normal Probability Plot

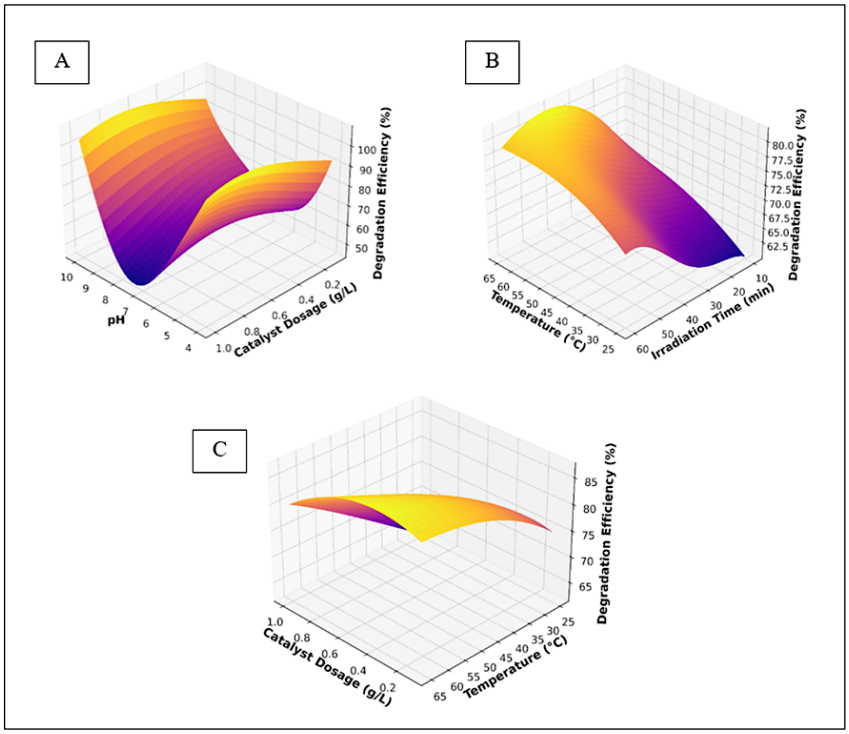

Figure 10: 3D Surface Plots for: A) pH vs Catalyst Dosage, B) Temperature vs Irradiation Time, C) Catalyst Dosage vs Temperature

3D Response Surface Plots and Interaction Analysis

The solution space of interaction effect of major operating variables of ph, catalyst dosage, and temperature and irradiation time on a photocatalytic degradation efficiency of paracetamol using TiO_2-ZnO nanocomposite was analysed and visualized through response surface methodology (RSM). The developed 3D surface plots (Figures 10A-10C) are helpful to answer a question on the nonlinear nature of these variables and the synergistic effects of their interactions. Figure 10A represents the degradation performance with regard to pH and dose of catalyst. The surface clearly indicates the parabolic dependence on pH, the efficiency at the beginning increases and reaches its apex at pH of 67 and then goes down to large alkalinity. This tendency coincides with the well-documented electrostatic interaction of the pollutant and the photocatalyst surface, under which conditions optimum charge interactions and production of radicals are achieved in near-neutral pH environments. The dosage curve however exhibits initial increase in efficiency owing to growth of active sites but with a further loading of catalyst (> 0.75 g/L) aggregation, and scattering of lights occur and the efficiency slightly reduces due to poor penetration of light. Such effects are put in line with previous works on metal oxide photocatalysis, which point to the trade-off between surface area and conquest of photons. The interaction between irradiation time and temperature is shown in Figure-10B. The rate of degradation increases with temperature until approximately 50°C at which point the degradation appears to level off. The behaviour indicates enhanced mobility of charge carriers with heating, and increased rates of radical generation, and is also indicative of a limit, imposed by recombination or by heating inactivation at high temperatures. Irradiation time, instead, exhibits a particularly strong linear correlation, with the increased degradation that results with the increased exposure time represented by the correlation transferring to increased duration of catalyst activation and cumulative release of photonic energy. Documenting the behaviour of saturation mentioned above after 50-60 minutes, the system is close to steady-state degradation as available molecules of paracetamol are almost spent or the reaction kinetics are limiting. The multiplying effect of catalyst dosage and temperature is represented in Figure 10C. The exterior shows that at low dosages of the catalyst, temperature makes a more significant effect to improve efficiency of degradation. At elevated catalyst doses, however, the effect of thermal support is reduced beneficially and this is possibly because there was overlapping particle deposition and light shielding. The best is the intermediate zone where it is possible to take full advantage of synergetic thermal and catalytic effects in the absence of overwhelming aggregation or recombination (39). These response surface interactions confirm that experimental parameters can drive the variation of the response in a nonlinear fashion and therefore multi-parameter optimization cannot be underestimated. Visual analyses allow strong model fits and determine the best operation windows that maximize the degradation in a future scaling application or hybrid device (40).

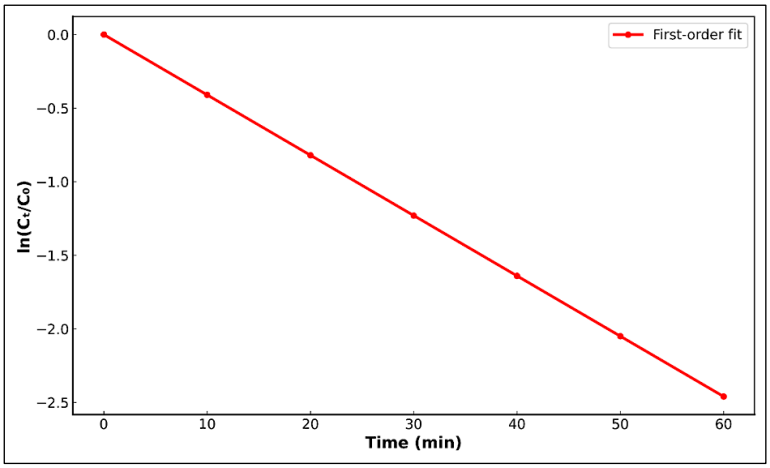

Figure 11: First-Order Kinetics Plot

Photocatalytic Kinetics

Kinetic analysis was used to obtain a deeper insight into the process of degradation of paracetamol under the resemblance of heat-assisted photocatalytic conditions with the first-order model since it is commonly used in heterogeneous photocatalysis. The degradation trend was assessed by graphically representing $\ln(C_t/C_0)$ of initial concentration C_0 and concentration after C_t (Figure 11). The plot of the data was linear and this is an indication that paracetamol degradation obeyed pseudo-first-order kinetics in the experiment conditions used. Using the slope of the regression line it was ascertained that the apparent rate constant (k) is about 0.041 min 1 which means that degradation rate is moderate, though quite effective. The strong correlation coefficient of Pearson (R^2 = 0.985) justifies the strength of this kinetic model to trace degradation trend as a function of time. The value of the kinetic constant is within the range of the normal values quoted in literature regarding the systems under UV-assisted degradation, based on TiO_2 or ZnO. The rate constant observed in this work is, however, slightly greater than those reported in previous studies that have not used any thermal integration, though, it means that there is a positive synergetic effect of heat on the mobility of charge carriers and also on the reaction kinetics. It could be suggested that such a high temperature in the experiment encouraged a higher rate of electron-hole production and increased the rate of the reactive oxygen species (ROS) formation including hydroxyl radicals and superoxide anions. Such ROS are important in initiating the attack of the paracetamol molecule especially during long irradiation. Also, the thermal energy could assist with minimizing electron-hole recombination, the greatest hindrance in semiconductor based photocatalysis, hence enhancing the net radical production and fastening degradation. That makes the plot very linear, showing that the rate of degradation was always dependent on the concentration of paracetamol at an instance in the experiment and never passed into the saturation (lag) period. It is instrumental behaviour in real-life application where uniform pollutant load is anticipated and eases the scaling of reactors. It also follows that secondary effects which are intermediate accumulation, catalyst deactivation or variation in brightness were also not substantive at the set operating condition (41). The rate constants in other studies of more single oxide systems or unassisted photocatalyzed reactions are reported as 0.01-0.035 min^{-1}. Incremental activity in this research proves the applicability of integrating TiO_2 and ZnO nanostructures in conjunction with the thermal support in the enhancement of photocatalytic kinetics. Thus, the incorporation of the heat to the photocatalytic system does not affect efficiency in degradation capacity in the photocatalytic system only, but also quantitatively enhances the rate of degradation rate, which is an important parameter in high throughput water treatment systems (42).

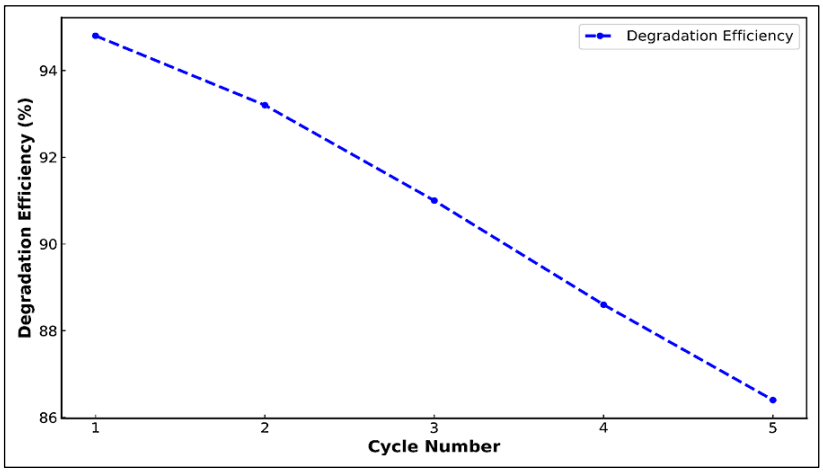

Figure 12: Reusability Curve

Catalyst Stability and Reusability

The effective determination of the practical viability of photocatalysts as applied in waste water treatment is based on measurement of reusability and long-term stability of the given photocatalyst. In this regard, five sequential

photocatalytic cycles were carried out at optimum operating conditions on TiO_2-ZnO the nanocomposite. Photocatalyst was recovered after each cycle by centrifugation, washed extensively in deionized water, dried and reused without further regeneration or heat treatment. Figure 12 is presented as the efficiency of degradation of each cycle. The %age efficiency during the initial cycle of the nanocomposite was found to be 94.8% which was dropping steadily to 86.4% in the fifth cycle and the overall loss of efficiency in the completion of reuse was estimated to be around 8.4%. This slow decrease means that the catalysts are fairly inert, yet it also suggests there are issues with minor deactivation in the course of time. This degradation tendency might occur due to a combination of a number of reasons, such as limited availability of active material in the recovered catalyst or diffusion of intermediates on the catalyst surface, changes in morphology and composition on the nanoparticle surface caused by repeated exposure to UV energy and high temperatures. The negative cumulative tendency of performance during the five cycles is within a margin of acceptability when compared with other photo thin film nanocomposites photocatalysts reported in previous researches. This structural and chemical stability is evidenced by the fact that in certain single component catalysts efficiency can reduce to 15-20% during comparable cycling times. The two oxides have synergistic effect on the overall activity retention, which is probably due to the preservation of the surface structure, and to the decrease in the creation of the re-combination centres under long-range irradiation. Additionally, the existence of both TiO_2 and ZnO together might promote better charge separation causes as well as the decreased recombination of electrons and holes so that, once partially deactivated, catalytic reactions may still occur. Potential elimination of sorbed intermediate residuals resulting could also be increased due to the work of the thermal energy during the actual reaction phase by stimulating surface regeneration, thus further life-span improvement of the catalyst. But to even improve reusability further, post-cycle mild annealing or solvent cleaning steps can be introduced into new regeneration protocols. In terms of operations, the economic and environmental viability of the catalyst to maintain more than 90% of its initial efficiency in the three cycles without ushering a chemical reactivation indicates some potential. This is important in an industrial setting where regeneration of catalysts is expensive in terms of costs and labour. The limited depreciation also proves the nanocomposites work as well as relates to their structure and the strength in degrading or loss in reaction to photo dissolution or leaching during experiment. On the whole, these findings indicate that TiO_2 -ZnO photocatalyst synthesized provides a fine balance between activity and reusability. These results support the possibility of this nanocomposite in long-term and repetitive application in continuous flow or batch characterized photocatalytic systems.

Conclusion

The current research reported the controllable design and performance assessment of a heat-assisted photocatalytic system using TiO_2 -ZnO nanocomposites on the degradation of a pharmaceutical wastewater using a paracetamol as a model drug. Synthesis of nanocomposite through sol-gel method produced a crystalline product with strong anatase and wurtzite phases as discovered by XRD and a homogenous nanoscale shape as shown by SEM. BET analysis revealed extremely high specific surface area (SSA) of 56.2 m^2/g and UV-Vis DRS analysis demonstrated low optical band gap of 2.84 eV which means visible light absorption increased and charge separation process improved. With the thermally integrated photocatalytic experiment, the maximum degradation %age obtained was 94.8 after 55 minutes of irradiation and an optimum pH of 5.8 and catalyst dosage of 0.9 g/L. The degradation kinetics was confirmed as first-order behaviour with a rate constant (k) of 0.041 min 1 at an optimal temperature of 50°C. When in comparison to photocatalysis of without heat input (efficiency of 81.2%), the temperature sensitivity in the application of heat came out strongly as 13.6 % efficiency improvement in the degradation process underlining temperature in increasing radical generation and charge mobility. The Box Behnken design based on RSM is statistically robust, as limited by the ANOVA and presented the positive value of the regression coefficient (R^2) at 0.985, and insignificance of the lack-of-fit ($p > 0.05$) that confirms the accuracy of the model predictions. 3D surface response plots showed critical importance of PH-catalyst dosage and time-

temperature interactions in response to degradation effectiveness. Reusability test on five successive cycles has simplicity showed that the nanocomposite sample maintained its activity as the degradation efficiency showed a slight drop in reduction of 94.8 to 86.4 which means that only 8.4 % has been lost, thus validating the structural and catalytic stability of nanocomposites. Compared to other documented systems that include pure TiO_2 (78.2%), ZnO (81.5%) and TiO_2 Fe_2O_3 (87.6%), TiO_2-ZnO nanocomposite was better in both activity and operating stability. The results reveal TiO_2-ZnO nanocomposite as an eccentrically active, temperature-stable, and reusable photocatalyst applicative in drug overrun waste water cleanup. Combination of thermal energy has the significant effect of enhancing photocatalytic activity and RSM optimization guarantees a high work level with minimum input in the operation. The work opens the path to scaling-up to pilot or industrial and the future work can be dedicated to coupling solar thermal inputs and degradation of complex pollutant blends.

Abbreviations

ANOV: Analysis of Variance, BET: Brunauer–Emmett–Teller Surface Area Analysis, CCD: Central Composite Design, DOE: Design of Experiments, FTIR: Fourier-Transform Infrared Spectroscopy, RSM: Response Surface Methodology, SEM: Scanning Electron Microscopy, TiO_2: Titanium Dioxide, UV–Vis DR: Ultraviolet–Visible Diffuse Reflectance Spectroscopy, XRD: X-ray Diffraction.

Acknowledgement

The authors would like to express their sincere gratitude to Hindusthan College of Engineering and Technology, Coimbatore for providing the necessary facilities and support to carry out this research work.

Author Contributions

Kavitha Subramanian: conceptualization, methodology, investigation, formal analysis, writing – original draft, visualization, project administration, Monica Silvenas Arulanthu Antony: supervision, writing – review & editing, data curation, validation, resources, funding acquisition, Arumugam Gopal: software, statistical analysis, visualization, writing – review, editing, Saravanan Jaganathan: investigation, experimental validation, materials preparation, methodology, data curation.

Conflict of Interest

The authors declare that there is no conflict of interest regarding the publication of this paper.

Data Availability

The data are available from the corresponding author upon reasonable request.

Declaration of Artificial Intelligence (AI) Assistance

The authors declare that no generative AI or AI-assisted technologies were used in the Writing, preparation, or editing of this manuscript.

Ethics Approval

This study does not involve human participants or animals. Therefore, ethical approval was not required.

Funding

This research did not receive any specific grant from funding agencies in the public, commercial, or not-for-profit sectors.

References

1. Samaei SM, Gato-Trinidad S, Altaee A. The application of pressure-driven ceramic membrane technology for the treatment of industrial wastewaters – A review. Sep Purif Technol. 2018;200:198–220. doi: 10.1016/j.seppur.2018.02.041
2. Ekblad M, Juárez R, Falås P, *et al*. Influence of operational conditions and wastewater properties on the removal of organic micropollutants through ozonation. J Environ Manage. 2021;286:112205. doi: 10.1016/j.jenvman.2021.112205
3. Audino F, Arboleda J, Petrovic M, *et al*. Pharmaceuticals removal by ozone and electro-oxidation in combination with biological treatment. Water (Basel). 2023;15(18):3180. doi: 10.3390/w15183180
4. Bagchi S, Behera M. Pharmaceutical wastewater treatment in ceramic separator MFC: Optimisation of operating parameters to improve organic removal and power generation. Clean Circ Bioecon. 2023;6:100063. https://doi.org/10.1016/j.clcb.2023.100063
5. Dalecka B, Strods M, Cacivkins P, *et al*. Removal of pharmaceutical compounds from municipal wastewater by bioaugmentation with fungi: An emerging strategy using fluidized bed pelleted bioreactor. Environ Adv. 2021;5:100086. doi: 10.1016/j.envadv.2021.100086
6. Hussein Al-Timimi DA, Alsalhy QF, AbdulRazak AA, *et al*. Optimum operating parameters for PES nanocomposite membranes for mebeverine hydrochloride removal. J Mater Res Technol.

2023;24:6779–90.
doi: 10.1016/j.jmrt.2023.04.247
7. Goswami RK, Agrawal K, Verma P. An exploration of natural synergy using microalgae for the remediation of pharmaceuticals and xenobiotics in wastewater. Algal Res. 2022;64:102703.
doi: 10.1016/j.algal.2022.102703
8. Sharma K, Kaushik G, Thotakura N, *et al*. Enhancement effects of process optimization technique while elucidating the degradation pathways of drugs present in pharmaceutical industry wastewater using *Micrococcus yunnanensis*. Chemosphere. 2020;238:124689.
doi: 10.1016/j.chemosphere.2019.124689
9. Ganthavee V, Trzcinski AP. Removal of pharmaceutically active compounds from wastewater using adsorption coupled with electrochemical oxidation technology: A critical review. J Ind Eng Chem. 2023;126:20–35.
doi: 10.1016/j.jiec.2023.06.003
10. Chakraborty S, Loutatidou S, Palmisano G, *et al*. Photocatalytic hollow fiber membranes for the degradation of pharmaceutical compounds in wastewater. J Environ Chem Eng. 2017;5(5):5014–24.
doi: 10.1016/j.jece.2017.09.038
11. Akkari M, Aranda P, Belver C, *et al*. ZnO/sepiolite heterostructured materials for solar photocatalytic degradation of pharmaceuticals in wastewater. Appl Clay Sci. 2018;156:104–9.
doi: 10.1016/j.clay.2018.01.021
12. Slimani Y, Almessiere MA, Mohamed MJS, *et al*. Synthesis of Ce–Sm co-doped TiO_2 nanoparticles with enhanced photocatalytic activity for Rhodamine B dye degradation. Catalysts. 2023;13(4):668.
doi: 10.3390/catal13040668
13. De Ceglie C, Pal S, Murgolo S, *et al*. Investigation of photocatalysis by mesoporous titanium dioxide supported on glass fibers as an integrated technology for water remediation. Catalysts. 2022;12(1):41.
doi: 10.3390/catal12010041
14. Sharifi Teshnizi M, Karimi M. TiO_2/graphene composite nanofibers for efficient photocatalytic degradation of pharmaceutical compounds: Rifampin, phenazopyridine, azathioprine. Environ Sci Pollut Res. 2023;30(49):108321–34.
doi: 10.1007/s11356-023-29869-9
15. Das S, Ahn Y-H. Synthesis and application of CdS nanorods for LED-based photocatalytic degradation of tetracycline antibiotic. Chemosphere. 2022;291(2):132870.
doi: 10.1016/j.chemosphere.2021.132870
16. Márquez G, Rodríguez EM, Maldonado MI, *et al*. Integration of ozone and solar TiO_2-photocatalytic oxidation for the degradation of selected pharmaceutical compounds in water and wastewater. Sep Purif Technol. 2014;136:18–26.
doi: 10.1016/j.seppur.2014.08.024
17. Phan HNQ, Leu HJ, Nguyen VND. Enhancing pharmaceutical wastewater treatment: Ozone-assisted electrooxidation and precision optimization via response surface methodology. J Water Process Eng. 2024;58:104782.
doi: 10.1016/j.jwpe.2024.104782
18. Zhang C, Huang J. Optimization of process parameters for pharmaceutical wastewater treatment. Pol J Environ Stud. 2015;24(1):391–5. https://doi.org/10.15244/pjoes/27866
19. Bajpai M, Katoch SS, Kadier A, *et al*. Treatment of pharmaceutical wastewater containing cefazolin by electrocoagulation (EC): Optimization of various parameters using response surface methodology (RSM), kinetics and isotherms study. Chem Eng Res Des. 2021;176:254–66.
doi: 10.1016/j.cherd.2021.10.012
20. Zango ZU, Lawal MA, Usman F, *et al*. Promoting the suitability of graphitic carbon nitride and metal oxide nanoparticles: A review of sulfonamides photocatalytic degradation. Chemosphere. 2024; 351:141218.
doi: 10.1016/j.chemosphere.2024.141218
21. Van Nuijs ALN, Tarcomnicu I, Simons W, *et al*. Optimization and validation of a hydrophilic interaction liquid chromatography–tandem mass spectrometry method for the determination of 13 top-prescribed pharmaceuticals in influent wastewater. Anal Bioanal Chem. 2010;398:2211–22.
doi: 10.1007/s00216-010-4101-1
22. Safo K, Noby H, Mitsuhara M, *et al*. Novel solar simulated photocatalytic heterolysis of pharmaceutical wastewater via slag nanocomposite immobilization: Optimization using response surface methodology. Water Pract Technol. 2023;18(10):2315–28.
doi: 10.2166/wpt.2023.152
23. Wang G, Wang D, Xu Y, *et al*. Study on optimization and performance of biological enhanced activated sludge process for pharmaceutical wastewater treatment. Sci Total Environ. 2020;739:140166.
doi: 10.1016/j.scitotenv.2020.140166
24. Zhang G, Huang X, Ma J, *et al*. Ti/RuO_2–IrO_2–SnO_2 anode for electrochemical degradation of pollutants in pharmaceutical wastewater: Optimization and degradation performances. Sustainability (Switzerland). 2021;13(1):126.
doi: 10.3390/su13010126
25. Kumar A, Shrivastava S, Tabassum A, *et al*. Optimization for removal of COD and BOD through RSM-CCD by activated sludge treatment process for pharmaceutical wastewater. J Environ Nanotechnol. 2023;12(4):68–86.
doi: 10.13074 / jent. 2023. 12.234486
26. Al-Khadhuri A, Al-Sabahi J, Kyaw HH, *et al*. Photocatalytic degradation toward pharmaceutical pollutants using supported zinc oxide nanorods catalyzed visible light system. Int J Environ Sci Technol. 2023;20(9):10021–30.
doi: 10.1007/s13762-022-04705-8
27. Kanakaraju D, Glass BD, Oelgemöller M. Titanium dioxide photocatalysis for pharmaceutical wastewater treatment. Environ Chem Lett. 2014;12:27–47.
doi: 10.1007/s10311-013-0428-0
28. Kar P, Aggarwal D, Shukla K, *et al*. Defect state modulation of TiO_2 nanostructures for photocatalytic abatement of emerging pharmaceutical pollutant in wastewater effluent. Adv Energy Sustain Res. 2021;3(5):2100162.
doi: 10.1002/aesr.202100162

29. Pérez-Lucas G, Aatik AE, Aliste M, *et al*. Removal of contaminants of emerging concern from a wastewater effluent by solar-driven heterogeneous photocatalysis: A case study of pharmaceuticals. Water Air Soil Pollut. 2023;234:60. doi:10.1007/s11270-023-06075-4
30. Joshi NC, Gururani P, Gairola SP. Metal oxide nanoparticles and their nanocomposite-based materials as photocatalysts in the degradation of dyes. Bioint Res Appl Chem. 2022;12(5):6557–79. doi: 10.33263/BRIAC125.65576579
31. Rekhate CV, Srivastava JK. Recent advances in ozone-based advanced oxidation processes for treatment of wastewater – A review. Chem Eng J Adv. 2020; 3:100031. doi: 10.1016/j.ceja.2020.100031
32. Kusmierek E. A CeO_2 semiconductor as a photocatalytic and photoelectrocatalytic material for the remediation of pollutants in industrial wastewater: A review. Catalysts. 2020;10(12):1435. https://doi.org/10.3390/catal10121435
33. Balarak D, Mostafapour FK. Photocatalytic degradation of amoxicillin using UV/synthesized NiO from pharmaceutical wastewater. Indones J Chem. 2019;19(1):211–8. https://doi.org/10.22146/ijc.33837
34. Noroozi R, Gholami M, Oskoei V, *et al*. Fabrication of new composite $NCuTiO_2$/CQD for photocatalytic degradation of ciprofloxacin and pharmaceutical wastewater treatment: Degradation pathway and toxicity assessment. Sci Rep. 2023; 13:42922. doi: 10.1038/s41598-023-42922-4
35. Teixeira S, Gurke R, Eckert H, *et al*. Photocatalytic degradation of pharmaceuticals present in conventionally treated wastewater by nanoparticle suspensions. J Environ Chem Eng. 2016;4(1):287–92. doi: 10.1016/j.jece.2015.10.045
36. Rejeb O, Yousef MS, Ghenai C, *et al*. Investigation of a solar still behaviour using response surface methodology. Case Stud Therm Eng. 2021;24:100816. doi: 10.1016/j.csite.2020.100816
37. Ling Z, Cao J, Zhang W, *et al*. Compact liquid cooling strategy with phase change materials for Li-ion batteries optimized using response surface methodology. Appl Energy. 2018;228:777–88. doi: 10.1016/j.apenergy.2018.06.143
38. Yuvaperiyasamy M, Senthilkumar N, Deepanraj B, *et al*. Application of response surface methodology and neural networks in pyramid solar still for seawater desalination: An optimization and prediction strategy. Glob NEST J. 2024;26(4):1-11. doi: 10.30955/gnj.005773
39. Kusakana K. Optimal energy management of a grid-connected dual-tracking photovoltaic system with battery storage: Case of a microbrewery under demand response. Energy. 2020;212:118782. doi: 10.1016/j.energy.2020.118782
40. Dolatabadi M, Ahmadzadeh S. A rapid and efficient removal approach for degradation of metformin in pharmaceutical wastewater using electro-Fenton process; optimization by response surface methodology. Water Sci Technol. 2019;80(4):685–694. doi: 10.2166/wst.2019.312
41. Lourens A, Falch A, Malgas-Enus R. Magnetite immobilized metal nanoparticles in the treatment and removal of pollutants from wastewater: A review. J Mater Sci. 2023;58:2951–70. doi: 10.1007/s10853-023-08167-2
42. Nezhad MA, Talaiekhozani A, Mojiri A, *et al*. Photocatalytic removal of ceftriaxone from wastewater using TiO_2/MgO under ultraviolet radiation. Environ Res. 2023;229:115915. doi: 10.1016/j.envres.2023.115915

How to Cite: Kavitha S, Antony MSA, Gopal A, Jaganathan S. Heat-assisted Photocatalytic Degradation of Pharmaceutical Wastewater Using TiO_2–ZnO Nanocomposites: Response Surface Optimization and Performance Evaluation. Int Res J Multidiscip Scope. 2026; 7(2): 1013-1032.
DOI: 10.47857/irjms.2026.v07i02.08183